

LOCALIZATION AND VISUALIZATION OF LOW-FREQUENCY ELECTROMAGNETIC SOURCES

K. Ishibana¹, S. Yagitani¹, I. Nagano¹, M. Kawauchi¹,
Y. Yoshimura², H. Hayakawa³, K. Tsuruda³

¹Graduate School of Natural Science and Technology, Kanazawa University

²Industrial Research Institute of Ishikawa

³Institute of Space and Astronautical Science, Japan Aerospace Exploration Agency

E-mail: ishibana@reg.is.t.kanazawa-u.ac.jp

Abstract: It is important to determine the location of electromagnetic noise sources within the electrical and electronic equipment under real operating conditions, to reduce the undesired noise emissions from the equipment. In this work we develop a system to locate electromagnetic sources, especially low-frequency (< MHz) magnetic dipoles (current loops), by measuring the magnetic field distributions around the sources. We apply the MUSIC algorithm to estimate both the locations and orientations of the incoherent multiple current loops. With simulations and experiments we evaluate the performance and accuracy of the MUSIC algorithm. We then visualize the estimated sources superimposed on the actual camera image of the sources.

Keywords: Low frequency, magnetic dipoles, current loops, MUSIC algorithm, Localization, Visualization

1. Introduction

To reduce the undesired electromagnetic (EM) noise emissions from the electrical and electronic equipment, it is important to identify the locations of EM noise sources within it. For the equipment under real operating conditions, we need to estimate the source locations inversely from the EM fields observed around it.

For high frequencies (more than hundreds of MHz), the EM sources at finite distances have been located for example with holographic imaging [1], estimation of current distributions based on CISPR measurement system [2], and the MUSIC algorithms [3][4][5]. On the other hand, at very low frequencies, the problem of localizing near-field EM sources has been solved for example in bioelectromagnetic inversion problems, such as the localization of the current dipoles within human brains [6]. The use of the MUSIC algorithm to characterize the near-field sources has also been discussed in a more general way [7].

In this study, we apply the MUSIC algorithm to localize the low-frequency (< MHz) magnetic dipoles (current loops), on the basis of the EM

near-field measurements with an array of magnetic vector sensors. We then develop a system to localize and visualize the locations and orientations of low-frequency current loops.

2. MUSIC Algorithm

2.1 Field measurement model

Here we apply the MUSIC algorithm [8] to estimate the 3-d locations and orientations of the low-frequency magnetic dipoles. For such a non-linear optimization problem the MUSIC algorithm can give an efficient and high-resolution estimation, with only a single dipole search over the 3-d space [6].

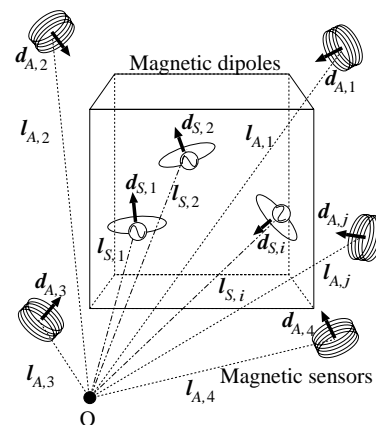


Figure 1: Magnetic dipole sources and magnetic sensors

As shown in Fig. 1, we have N_S incoherent source magnetic dipoles at arbitrary locations $l_{S,i}$ and orientations $d_{S,i}$ ($i = 1, 2, \dots, N_S$). The source signals $s_i(t)$ input to the dipoles are assumed to be narrowband, and the locations and orientations of the dipoles do not change during measurement. The magnetic field distribution radiated from the source dipoles is measured by N_A magnetic sensors whose locations and orientations given by $l_{A,j}$ and $d_{A,j}$, ($j = 1, 2, \dots, N_A$). Here the number of sensors N_A should be larger than the number of sources N_S .

The magnetic field waveform at the j -th sensor is written as $x_j(t) = \sum_{i=1}^{N_S} a_{ji} s_i(t) + n_j(t)$, where $n_j(t)$ is the additive noise being zero mean and white with variance σ . Here the steering vector component a_{ji} depends nonlinearly on the distance between the j -th sensor and the i -th source, as well as on their orientations.

2.2 MUSIC estimation of source parameters.

With the eigenanalysis of the covariance matrix \mathbf{R}_{xx} calculated from the measured magnetic field vector $\mathbf{X}(t)$, we have $N_A - N_S$ noise eigenvalues. The space \mathbf{E}_N spanned by the corresponding eigenvectors are orthogonal to the steering vector for the true sources, $\mathbf{a}_i(\mathbf{l}_{S,i}, \mathbf{d}_{S,i})$, so that we can determine the source locations and orientations, by evaluating the local maxima of the MUSIC cost function P_{music} , given as,

$$P_{music}(\mathbf{l}, \mathbf{d}) = \frac{\|\mathbf{a}(\mathbf{l}, \mathbf{d})\|^2}{\|\mathbf{E}_N^H \mathbf{a}(\mathbf{l}, \mathbf{d})\|^2} \quad (1)$$

where H means the Hermitian conjugate. Here $\mathbf{a}(\mathbf{l}, \mathbf{d})$ represents the steering vector for the location \mathbf{l} and orientation \mathbf{d} of the dipole sources.

To search for the local maxima of P_{music} with (1), we may have to impractically scan all of the possible combinations among the locations \mathbf{l} and the orientations \mathbf{d} of the source dipoles. However, it turns out that we can scan only the locations \mathbf{l} , to estimate both the locations and orientations of the dipoles. We decompose the steering vector into the elementary steering vectors \mathbf{a}_x , \mathbf{a}_y , and \mathbf{a}_z , which correspond to x , y , and z -directed source dipoles, respectively [6][9], as $\mathbf{a}(\mathbf{l}, \mathbf{d}) = [\mathbf{a}_x | \mathbf{a}_y | \mathbf{a}_z] \mathbf{d} \equiv \mathbf{a}_{xyz} \mathbf{d}$, where we have defined $\mathbf{a}_{xyz} \equiv [\mathbf{a}_x | \mathbf{a}_y | \mathbf{a}_z]$. From this, the cost function P_{music} can be modified as the function of only the locations \mathbf{l} , as

$$P_{music}(\mathbf{l}) = \frac{\mathbf{e}_{min}^H \mathbf{a}_{xyz}^H \mathbf{a}_{xyz} \mathbf{e}_{min}}{\lambda_{min} \left(\mathbf{a}_{xyz}^H \mathbf{E}_N \mathbf{E}_N^H \mathbf{a}_{xyz} \right)} \quad (2)$$

where $\lambda_{min}(\cdot)$ means to take the minimum eigenvalue of the matrix in the parenthesis. The modified cost function $P_{music}(\mathbf{l})$ takes maximum at each of true source dipole locations, where the eigenvector \mathbf{e}_{min} corresponding to the minimum eigenvalue represents the orientation of the dipole.

We can further save the MUSIC search by interpolating the true source locations from sparsely distributed scanning points [10]. Around each of the local maxima of P_{music} evaluated at the sparse 3-d grid points, we select the four grid points which are not on the same plane, \mathbf{l}_j ($j = 1, 2, 3, 4$). We assume that the denominator of P_{music} , defined as \mathbf{v} , varies linearly over these grid points.

Defining

$$[\mathbf{v}_{xj} | \mathbf{v}_{yj} | \mathbf{v}_{zj}] \equiv \mathbf{E}_N^H [\mathbf{a}_x(\mathbf{l}_j) | \mathbf{a}_y(\mathbf{l}_j) | \mathbf{a}_z(\mathbf{l}_j)] \quad (3)$$

we calculate $\mathbf{v}_j \equiv \mathbf{v}_{xj} \wedge \mathbf{v}_{yj} \wedge \mathbf{v}_{zj}$, where \wedge is a wedge product. The linear combination of \mathbf{v}_j should become zero at the true source location so that

$$[\mathbf{v}_1 | \mathbf{v}_2 | \mathbf{v}_3 | \mathbf{v}_4] \mathbf{c} = \mathbf{v}_0 \cong 0 \quad (4)$$

where the coefficient vector \mathbf{c} is normalized as $[1 \ 1 \ 1 \ 1] \mathbf{c} = 1$. Solving (4) for \mathbf{c} , we can interpolate the true source location \mathbf{l}_0 , by

$$\mathbf{l}_0 = [\mathbf{l}_1 | \mathbf{l}_2 | \mathbf{l}_3 | \mathbf{l}_4] \mathbf{c}. \quad (5)$$

Note that combining this interpolation with (2), the maximum number of estimated sources N_S is reduced down to $N_A - 4$.

2.3 Simulation

We have performed a couple of simulations, to demonstrate the validity of the MUSIC algorithm developed in the previous section. By using three magnetic vector sensors at the locations $(x, y, z) = (0, 0, 0), (1, 0, 0), (2, 0, 0)$ [m], we have tried to localize two incoherent magnetic dipoles at the frequencies of 10 kHz and 10.5 kHz, respectively, with arbitrary locations and orientations. When the SNR of the measured signals are as good as more than 30 dB, the location accuracy (the rms error variance) has confirmed to become less than 1 mm at the locations about 1 m away from the sensor array. As the distance between the sources and the sensor increases, the estimation error variance increases up to centimeters because of the reduced SNR. In addition to such rms error variation, another ‘‘bias error’’ of the MUSIC algorithm appears in the estimated locations. Though the MUSIC estimator itself is an ‘‘unbiased’’ estimator, here the bias error comes from the interpolation scheme shown in (5) [10]. For the MUSIC scanning resolution of 10 cm over the 3-d volume including the sources, this bias error makes the estimated locations deviate by up to centimeters from the true source locations, which can be reduced if we adopt finer scanning resolution.

3. Location and visualization experiment for low-frequency current loops

We have developed an experimental system to locate and visualize the low-frequency current loop sources as in Fig. 2, with the MUSIC algorithm. As an example of the experiments, we set up two small current loops with diameters of about 10 cm. As in the simulation the current loop sources #1 and #2 have the monochromatic frequencies at 10 kHz and 10.5 kHz with the dipole moments

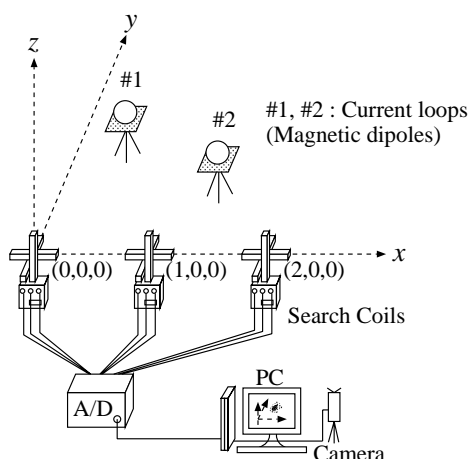


Figure 2: Experiment configuration for low-frequency current loop visualization

of 6.3×10^{-3} A/m and 1.8×10^{-3} A/m, respectively. Their locations and orientations are listed as the “True” values in Table 1, where the orientations are represented as the zenith angle θ from the z -axis and the azimuth angle ϕ from the x -axis.

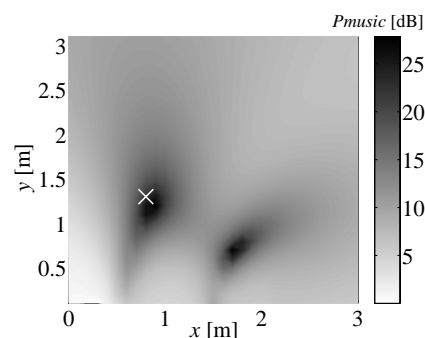
Again as in the simulation we put three tri-axial search coil sensors at $(0, 0, 0)$, $(1, 0, 0)$, and $(2, 0, 0)$ [m]. These sensors have been developed to observe the weak electromagnetic waves in space plasmas around the Earth onboard scientific satellites [11]. The wave forms of the measured magnetic field are sampled at 200 kHz.

The MUSIC scan is done over the $3 \text{ m} \times 3 \text{ m} \times 3 \text{ m}$ volume including the sources, with the resolution of 10 cm, where the SNR for the sources #1 and #2 are 36.2 dB and 31.0 dB, respectively.

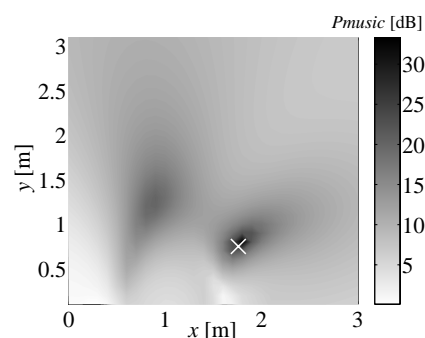
Figs. 3(a) and (b) show the P_{music} distributions over two $x - y$ (horizontal) plane at $z = 0.1 \text{ m}$ and $z = -0.1 \text{ m}$, for the sources #1 and #2, respectively. The “ \times ” marks in the figures indicate the true locations of the sources, which agree with two local maxima of P_{music} . The exact values of estimated locations with interpolation are listed as “Estimated” in Table 1. In this case the estimation error becomes as large as about 10 cm for the location, which is larger than not only the rms error variance due to the noise but also the bias error

Table 1: Source parameters

	Location [m]	Orientation (θ, ϕ) [deg]
#1:True	(0.80, 1.30, 0.00)	(0, 0)
#1:Estimated	(0.86, 1.19, 0.11)	(5, -126)
#1:True	(1.76, 0.75, 0.00)	(55, 45)
#2:Estimated	(1.77, 0.77, -0.07)	(59, 53)



(a) $z = 0.1 \text{ m}$



(b) $z = -0.1 \text{ m}$

Figure 3: Locations of the current loop sources estimated by the MUSIC algorithm

of the MUSIC estimator due to the interpolation. The main reason of this is likely to be attributed to the incorrect alignment of each axial sensor of the tri-axial search coils, as well as to the assumption of the finite-sized (10 cm diameter) current loop sources treated as “point” magnetic dipole sources.

With our system the estimated source locations and orientations can be superimposed directly on the “real” camera image of the loop currents, by adjusting the relationship between the camera coordinates and the real coordinates, on the basis of the camera parameters with perspective transformation. Fig. 4 shows a visualized result, where we draw two “ellipses” representing the two current loops as seen from the camera and two “arrows” indicating their orientations.

4. Conclusion

We have applied a MUSIC algorithm to localize the multiple incoherent low-frequency magnetic dipole sources. On the basis of the algorithm, we have developed a system to determine the locations and orientations of the current loops and visualize them on the real image of the sources.

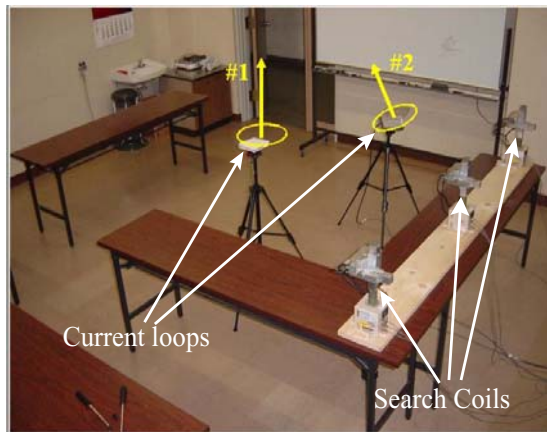


Figure 4: Visualization of low-frequency current loops

Since the algorithm developed here only treats point magnetic dipole sources (small current loops), we will extend the algorithm to deal with line and plane current sources, by possibly estimating their current distributions [12].

On the other hand, the actual EM noise sources inside electrical and electronic equipment may be surrounded by metal chassis or frames, which should influence the radiation and propagation of the noise out of the equipment. With the aid of computer simulation of EM wave propagation, we will evaluate such an effect and apply it to the localization and visualization of actual noise sources inside the equipment.

Acknowledgments

We wish to thank Messrs. S. Kato and Y. Nishi for their support in developing the experimental system. This work was mainly supported by Research Project “Control of Electromagnetics Environment in Low Frequency Band Less Than 100 kHz” of the Reclamation Research Promotion Business in the Future of Japan Society for the Promotion of Science (JSPS). Part of this work was also supported by the JSPS Grant-in-Aid for Scientific Research (Young Scientists (B), No. 14750287), and Takahashi Industrial and Economic Research Foundation. The experimental system was partly prepared by the Special Coordination Funds for Promoting Science and Technology (Leading Research Utilizing Potential of Regional Science and Technology) of the Ministry of Education, Culture, Sports, Science and Technology of the Japanese Government.

References

- [1] H. Kitayoshi, and K. Sawaya, “Electromagnetic-wave visualization for EMI using a new holographic method,” *Electron. Commun. Jpn. 1, Commun.*, vol. 82, no. 8, pp. 52–60, Aug. 1999.
- [2] Y. Ishida, Y. Yamaguchi, and M. Tokuda, “Visualization of radiated emission sources by estimating current values based on CISPR measurement system,” *Trans. IEICE*, vol. J84-B, no. 3, pp. 570–581, Mar. 2001. (in Japanese)
- [3] Y. -D. Huang, and M. Barkat, “Near-field multiple source localization by passive sensor array,” *IEEE Trans. Antennas and Propagation*, vol. 39, no. 7, pp. 968–975, Jul. 1991.
- [4] K. Taira, T. Kato, and K. Sawaya, “Estimation of short range electromagnetic source location using the estimation method for direction of arrival —Experimental study—,” *Technical Report of IEICE*, AP2002-48, pp. 49–54, Jul. 2002.
- [5] A. Ohmae, M. Takahashi, and T. Uno, “Localization of sources in the finite distance using MUSIC Algorithm by the spherical mode vector,” *Technical Report of IEICE*, AP2003-64, pp. 139–142, Jul. 2003.
- [6] J. C. Mosher, P. S. Lewis, and R. M. Leahy, “Multiple dipole modeling and localization from spatio-temporal MEG data,” *IEEE Trans. Biomedical Engineering*, vol. 39, no. 6, pp. 541–557, Jun. 1992.
- [7] B. Audone, and M. B. Margari, “The use of MUSIC algorithm to characterize emissive sources,” *IEEE Trans. Electromagnetic Compatibility*, vol. 43, no. 4, pp. 688–693, Nov. 2001.
- [8] R. O. Schmidt, “Multiple emitter location and signal parameter estimation,” *IEEE Trans. Antenna and Propagation*, vol. AP-34, no. 3, pp. 276–280, Mar. 1986.
- [9] R. O. Schmidt, “Multiple source DF signal processing: an experimental system,” *IEEE Trans. Antennas and Propagation*, vol. AP-34, no. 3, pp. 281–291, Mar. 1986.
- [10] R. O. Schmidt, “Multilinear array manifold interpolation,” *IEEE Trans. Antenna and Propagation*, vol. 40, no. 4, pp. 857–866, Apr. 1992.
- [11] H. Matsumoto, H. Kojima, Y. Omura, and I. Nagano, “Plasma Waves in Geospace: GEOTAIL Observations,” *New Perspectives of the Earth’s Magnetotail*, A. Nishida, D. N. Baker, S. W. H. Cowley (eds.), AGU Monograph, 105, American Geophysical Union, Washington D.C., pp.261–322, Nov. 1998.
- [12] S. Valaee, B. Champagne, and P. Kabal, “Parametric localization of distributed sources,” *IEEE Trans. on Signal Processing*, vol. 43, no. 9, pp. 2144–2153, Sep. 1995.